Mon. Not. R. Astron. Soc. **000**, 000–000 (1998) Printed 17 July 2006 (MN LATEX style file v1.4)

Direct Calibration of the Cepheid Period-Luminosity relation ⋆

Lanoix P. [1,2], Paturel G. [1], Garnier R.[1]
[1] *CRAL-Observatoire de Lyon, F69230 Saint-Genis Laval, FRANCE,*
[2] *Université Claude Bernard Lyon I, F69622 Villeurbanne, FRANCE*

Received December 1998; accepted – – –

ABSTRACT
After the first release of HIPPARCOS data, Feast & Catchpole gave a new value to the zero-point of the visual Cepheid Period-Luminosity relation based on trigonometric parallaxes. Because of the large uncertainties on these parallaxes, the way in which individual measurements are weighted bears a crucial importance, and the discrepancy they show leads to the conclusion that the choice of the best weighting system can be provided through a Monte-Carlo simulation.
On the basis of such a simulation it is shown that:

- A cut in π or in σ_π/π introduces a strong bias.
- The zero-point is more stable when only the brightest Cepheids are used.
- The Feast & Catchpole weighting gives the best zero-point and the lowest dispersion.

After correction, the adopted visual Period-Luminosity relation is:

$$\langle M_V \rangle = -2.77 \log P - 1.44 \pm 0.05.$$

Moreover, we extend this study to the photometric I-band (Cousins) and obtain:

$$\langle M_I \rangle = -3.05 \log P - 1.81 \pm 0.09.$$

Key words: Cepheids – P-L Relation – Distance scale –

1 INTRODUCTION

Cepheid variables constitute one of the most important primary distance calibrators. Indeed, they obey a Period-Luminosity (PL) relation:

$$\langle M_V \rangle = \delta \ \log P + \rho \qquad (1)$$

from which the absolute magnitude $\langle M_V \rangle$ can be determined just from the measurement of the period, provided that the slope δ and the zero-point ρ are known.

The slope of the PL relation seems very well established from ground-based observations in the Large Magellanic Cloud (LMC) because the population incompleteness bias pointed out for more distant galaxies (Lanoix et al. 1999a) seems negligible in the LMC. The slope of the PL relation is easier to obtain from an external galaxy because, all Cepheids being at the same distance, the slope can be determined by using apparent magnitudes instead of absolute magnitudes. A reasonable value for the photometric V-band is $\delta = -2.77 \pm 0.08$ (see for instance Gieren et al. 1998, Tanvir 1997, Caldwell & Laney 1991, Madore & Freedman 1991). In the present study we will adopt this value and will discuss further the effect of a change of it.

The establishment of the zero-point still remains a major goal. Today, thanks to the HIPPARCOS satellite †, the trigonometric parallaxes of galactic Cepheids are accessible, allowing a new determination of ρ.

After the first release of HIPPARCOS data, a calibration of the Cepheid PL relation was published by Feast & Catchpole (1997, hereafter FC). This work gave a distance for the LMC galaxy larger than the one generally assumed. However, some papers (Madore & Freedman 1998, Sandage & Tammann 1998) argued that this calibration is only brighter than previous ones at the level of ≤ 0.1 mag. An independent study of the calibration of the PL relation based on the same data also led to a long distance scale (Pa-

⋆ Based on data from the ESA HIPPARCOS astrometry satellite

† HIPPARCOS parallaxes are ten times better than those obtained from ground-based observations (i.e., $\sigma_\pi \approx 1$ milliarcsec).

turel et al. 1996) and to a large LMC distance modulus of 18.7 (Paturel et al. 1997). All these studies may be affected by statistical biases due either to the cut of negative parallaxes or to the method used for bypassing these cuts. This justifies that we want to analyze deeper these results.

HIPPARCOS parallaxes π may have large standard deviations σ_π leading sometimes to negative parallax so that the distance d(pc)=$1/\pi$ cannot be calculated. Anyway, it is a biased estimate of the true distance (Brown et al. 1997). Thus, it seems impossible to use it for a direct calculation of the zero-point. On the other hand, rejecting negative parallaxes generates a Lutz-Kelker bias type (Lutz & Kelker 1973) while rejecting parallaxes with large σ_π/π generates another bias (Brown et al. 1997). In order to bypass this problem, FC suggest calculating ρ from the weighted mean of the function:

$$10^{0.2\rho} = 0.01\pi 10^{0.2(\langle V_0\rangle - \delta \log P)} \quad (2)$$

This treatment assumed that the exponent of a mean is identical to the mean of the exponents. FC justify it by saying that "the scatter about the PL(V) relation is relatively small". They chose a weighting and compute the mean of $10^{0.2\rho}$, from which they derive ρ.
As a matter of fact, they use a Period-Color (PC) relation for dereddening their magnitudes. Because of the near degeneracy of the reddening slope and the colour term in a Period-Luminosity-Color relation, this technique will have much the same narrowing effect on the PL relation as including a color term would. For a Cepheid of known distance the scatter is reduced from 0.2 down to about 0.1. However since the HIPPARCOS parallaxes may have large errors, we see from equation 2 that the scatter in $10^{0.2\rho}$ could be increased in this manner.

Precisely, we would like to answer the following questions:

- Can we obtain a good result by rejecting poor parallaxes?
- Is the dispersion small enough to justify the calculation of ρ using the mean of $10^{0.2\rho}$?
- Is the final result biased or not?
- Is it possible to adopt another weighting than that of FC?

In section 2 we use the HIPPARCOS sample of Cepheids to confirm that rejecting negative parallaxes or parallaxes with a poor σ_π/π gives a biased zero-point and to test the FC method with different weighting systems. This suggests making a simulated sample for which the zero-point is *a priori* known and then to apply the same treatment to it.

In section 3 we explain how the simulated sample is built in order to reproduce all the properties of the true HIPPARCOS sample.

Then, in section 4 we give the result of the FC method applied to the simulated sample with different weightings. This shows that the calculated zero-points and the associated standart deviations depend on the adopted weigthing.

In section 5, the previous results are discussed and explained. The consequences are drawn for estimating the best zero-point from the HIPPARCOS Cepheid sample for both V and I bands.

2 USE OF THE HIPPARCOS CEPHEID SAMPLE

The complete Cepheid sample is extracted from the catalogue HIPPARCOS (1997). Among all variable stars, we keep only those labelled DCEP (classical $\delta-$type Cepheids) and DCEPS (first overtone pulsators), and then obtained a total of 247 Cepheids. The period of the 31 overtone pulsators is converted to the fundamental period P according to Alcock et al. (1995):

$$P_1/P = 0.716 - 0.027 \log P_1 \quad (3)$$

The B and V photometry is available from the David Dunlap Observatory Galactic Cepheid Database (Fernie et al. 1995), except for nine Cepheids (CK Cam, BB Gem, KZ Pup, W Car, DP Vel, BB Her, V733 Aql, KL Aql and V411 Lac) which were excluded from the present study. Therefore, the final sample (table 4) is made of 238 Cepheids (31 overtones).

The color excess is then calculated using the FC method, i.e. calculation of the intrinsic color $\langle B\rangle_0 - \langle V\rangle_0$ from a linear relation color vs. $\log P$, according to Laney & Stobie (1994):

$$\langle B\rangle_0 - \langle V\rangle_0 = 0.416 \log P + 0.314. \quad (4)$$

We use the relation from Laney & Stobie (1993) to compute the V extinction :

$$R_V = 3.07 + 0.28(\langle B\rangle_0 - \langle V\rangle_0) + 0.04E_{(B-V)} \quad (5)$$

Figure 1 shows how the quantity $10^{0.2\rho}$ varies with the apparent magnitude V. This quantity is directly needed for the calculation of the zero-point ρ. Clearly, the dispersion increases with the magnitude, but the distribution is quite symetrical around a given value.

If a cut is applied on the sample to reject negative parallaxes (filled triangles in figure 1) the mean of $10^{0.2\rho}$ is overestimated. If one uses only measurements with $0 < \sigma_\pi/\pi < 0.5$ (open circles in figure 1), again, $10^{0.2\rho}$ is overestimated. Thus, as claimed by Brown et al. (1997), a bias is clearly confirmed if one cuts the sample. We will no more consider cuts involving parallaxes as a way of obtaining a valuable result.

Figure 1 does not exhibit a small dispersion. So, we do not know if the FC's procedure leads to the proper value of ρ. For the calculation of the mean of $10^{0.2\rho}$ they use individual weights taken as the reciprocal of the square of the standard error of the second term of equation 2. For a given Cepheid, the weight is given by:

$$\omega_i \approx [10^{-2}\sigma_{\pi_i} 10^{0.2(\langle V_{0_i}\rangle - \delta \log P_i)}]^{-2} \quad (6)$$

because the error on the term $10^{0.2(\langle V_{0_i}\rangle - \delta \log P_i)}$ is negligible as shown by FC. This weighting is mathematically the most rigorous. However, some other empirical weightings may be worthy of interest.

Since the error on ρ is mainly due to the large uncertainty σ_π, we will test a weight in $\sigma_{\pi_i}^{-2}$ and in $(\sigma_{\pi_i}/\pi_i)^{-2}$. Further, we will also use an unweighted mean because the dispersion looks quite symetrical around a mean value and a V^{-2} weighting because the dispersion increases with V. We then repeated the FC tests as well as the other weightings and found the results given in table 1.

From this table we see that, when all Cepheids are used, the calculated zero-point ρ strongly depends on the adopted

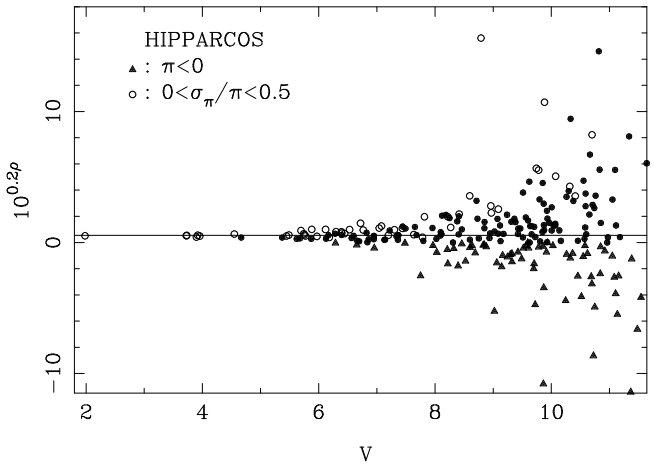

Figure 1. Effects of cuts. The horizontal line corresponds to the zero-point value $\rho = -1.43$. If one rejects negative parallaxes (filled triangles) or keeps parallaxes with $0 \leq \sigma_\pi/\pi \leq 0.5$ (open circles), the mean is overestimated.

Table 1. Values of ρ calculated with different weightings and different cuts in V magnitude. The standard deviation of each value is given in parenthesis.

Weighting	All V	$V \leq 8$	$V \leq 6$
F&C	−1.45(0.10)	−1.47(0.10)	−1.45(0.08)
$\sigma_{\pi_i}^{-2}$	−1.04(0.37)	−1.38(0.22)	−1.45(0.16)
$(\sigma_{\pi_i}/\pi_i)^{-2}$	1.19(0.57)	–	–
No weight	−0.19(0.74)	−1.38(0.22)	−1.40(0.17)
V^{-2}	−0.64(0.65)	−1.41(0.22)	−1.42(0.13)

weighting. The instability of this result can be explained by the very large dispersion at large V. This large dispersion quite justifies the second question of section 1.

According to the shape of figure 1, we see that the dispersion can be reduced by cutting the sample at a given apparent magnitude. Table 1 shows that such a cut gives a more stable result. Moreover, the weighting adopted by FC gives the lowest dispersion. For instance, keeping the brightest 11 Cepheids, we obtain $\rho = -1.45$ with a very small standard deviation of 0.05 ($V \leq 5.5$). We also try to keep only stars with the highest weights (whatever the weighting system). However, that leads us to the same results with slightly higher dispersions.

In practice, we have no means of knowing if a bias has been introduced as long as the observed sample is used because the true zero-point is not known. Only a simulated sample, with a zero-point *a priori* known, can provide the answer to the third question of section 1. This justifies the construction of simulated samples.

3 CONSTRUCTION OF SIMULATED SAMPLES

To build a simulated sample only three quantities have to be drawn independently:

- The parallax π
- The logarithm of the period $\log P$
- The column density of interstellar matter along the line of sight.

3.1 The simulated "true parameters"

Assuming a homogeneous 3D distribution of galactic Cepheids (this is justified owing to relatively small depth of HIPPARCOS survey regarding the depth of the galactic disk), we draw at random the x,y,z coordinates over the range [-2100, 2100] pc. We keep only Cepheids within a radius of 2100 pc and then deduce the true parallax:

$$\pi = 1/\sqrt{x^2 + y^2 + z^2} \tag{7}$$

250 true parallaxes are drawn in such a way. Each point will be a Cepheid in our simulated sample.
Then, for each Cepheid we draw $\log P$ following a distribution which reproduces the observed distribution of periods (Fig. 5a and 5b). We then calculate the absolute magnitude $\langle M_V \rangle$ from the relation:

$$\langle M_V \rangle = \delta_V \log P + \rho_V + \Delta \tag{8}$$

where $\delta_V = -2.77$ is the adopted slope as said in the introduction, $\rho_V = -1.30$ is the arbitrarily fixed zero-point and Δ is a Gaussian intrinsic dispersion ($\langle \Delta \rangle = 0$; $\sigma(\Delta) = 0.2$) which reflects the width of the instability strip. The absolute magnitude in B-band $\langle M_B \rangle$ is calculated in the same way using the same intrinsic dispersion multiplied by 1.4. We reproduce in this manner the correlation of the residuals as well as the dispersion of the true CP relation related to the color variation across the instability strip. We chose $\delta_B = \delta_V + 0.416$ and $\rho_B = \rho_V + 0.314$, so that it implies the relation between the intrinsic color $\langle B \rangle_0 - \langle V \rangle_0$ and $\log P$ from Laney & Stobie (1994):

$$\langle B \rangle_0 - \langle V \rangle_0 = (\delta_B - \delta_V) \log P + \rho_B - \rho_V \tag{9}$$

The true intrinsic color $\langle B \rangle_0 - \langle V \rangle_0$ is calculated from this linear relation. We then reduce the dispersion of the PL relation down to 0.1 as already explained in the introduction.

The relation of $E_{(B-V)}$ versus the calculated photometric distances (adopting, for instance, distances from Fernie et al. 1995) shows (Fig. 2) that the observed Cepheids are located in a sector. All line of sight directions have extinction (no point below the dashed line). In slightly obscured directions (dashed line) one can see stars up to ≈ 5000 pc, while in very obscured regions (dotted line) the closest Cepheids are detected not farther than ≈ 1100 pc.

The slope $E_{(B-V)}/distance$ is a measure of the density of the interstellar medium in a given direction. This density varies over a large range due to the patchiness of the galactic extinction, but, for a given line of sight, the extinction, and thus the color excess, is assumed to be proportional to the distance. This figure is used to obtain the extinction for each Cepheid. We draw at random the slope $E_{(B-V)}/distance$ over the range defined by the dashed and dotted lines (Fig. 2). Using the true distance $1/\pi$ we then deduce the true color excess $E_{(B-V)}$, and the true extinctions:

$$A_V = R_V E_{(B-V)} \tag{10}$$

$$A_B = R_B E_{(B-V)} \tag{11}$$

with $R_V = 3.3$ and $R_B = 4.3$.

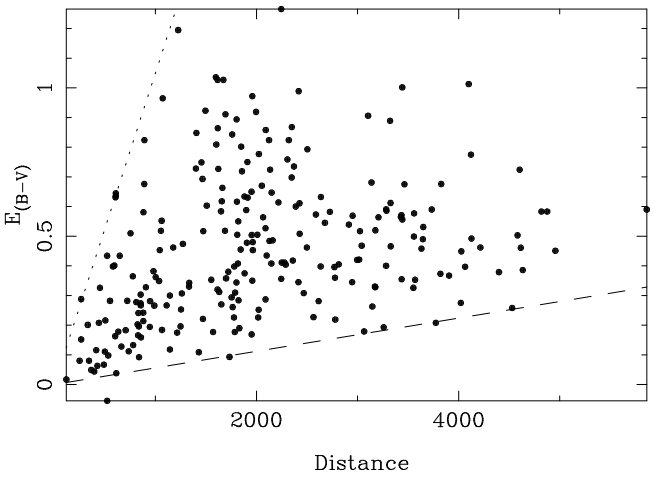

Figure 2. Color exces versus photometric distances from Fernie (Fernie et al. 1995) for HIPPARCOS Cepheids. The slope $E_{(B-V)}/distance$ measures the density of the interstellar medium. In slightly obscured directions (dashed line) one can see stars up to $\approx$ 5000 pc, while in very obscured regions (dotted line) the closest Cepheids are detected not farther than $\approx$ 1100 pc.

3.2 The simulated "observed parameters"

Now we calculate the parameters which would be observed. First, the apparent B and V magnitudes are simply:

$$\langle V\rangle = 5\log(1/\pi) - 5 + \langle M_V\rangle + A_V + \epsilon_V \quad (12)$$

$$\langle B\rangle = 5\log(1/\pi) - 5 + \langle M_B\rangle + A_B + \epsilon_B \quad (13)$$

where ϵ_V and ϵ_B are two independent Gaussian variables which reproduce measurement uncertainties (the intrinsic scatter of the PL relation is already counted in $\langle M_V\rangle$ and $\langle M_B\rangle$). We adopted for both: $\langle\epsilon\rangle = 0.0$ and $\sigma_\epsilon = 0.005$.

The parallax which would be observed is calculated from the true one and an associated σ_π obtained through the figure 11a. This figure shows two populations: one below the dotted line, the other about the dotted line. First, we draw the membership to one of these families in the right proportion. Then, from the linear relationships of the corresponding family and the V magnitude already computed, we calculate $\log\sigma_\pi$ (i.e. σ_π). Finally, the observed π is obtained by drawing one occurence in the Gaussian distribution (π, σ_π).
Concerning the observed color excess, it will simply be deduced from the relation:

$$E_{(B-V)} = \langle B\rangle - \langle V\rangle - (\langle B\rangle_0 - \langle V\rangle_0) \quad (14)$$

with $\langle B\rangle_0 - \langle V\rangle_0$ deduced from the PC relation 9 as we did in section 2.

We also need to determine the observed value of the coefficient R_V. We draw its value according to a Gaussian distribution centered on the chosen true value (3.3) with a dispersion of 0.05. So, we suppose that the observed value has no systematic shift with respect to the true value.

Finally, in order to reproduce selection effects like the Malmquist bias (Malmquist 1920) we reject the Cepheids which could not be observed according to their apparent magnitudes (i.e. their probability to be detected). We draw a random parameter $t \in [0, 1]$ and compute the quantity:

Table 2. Values of ρ calculated using 1000 simulated samples. We used different weightings and different cuts in V magnitude as in the study made with the true sample. The standard deviation of each value is given in parenthesis.

weighting	All V	$V \leq 8$	$V \leq 6$
true zero-point	−1.30	−1.30	−1.30
F&C	−1.31(0.14)	−1.30(0.15)	−1.31(0.21)
$\sigma_{\pi_i}^{-2}$	−1.33(0.21)	−1.31(0.22)	−1.31(0.26)
$(\sigma_{\pi_i}/\pi_i)^{-2}$	0.03(0.47)	–	–
No weight	−1.36(0.43)	−1.33(0.39)	−1.32(0.34)
V^{-2}	−1.33(0.33)	−1.32(0.32)	−1.31(0.29)

$$t_0 = \frac{1}{1+\exp^{\alpha(\langle V\rangle - \langle V_{lim}\rangle)}} \quad (15)$$

Whenever $t \leq t_0$ the star may be observed by HIPPARCOS and we keep it in our sample, and in the other case it will be rejected. We assume $\alpha = 1$ and $\langle V_{lim}\rangle = 12.5$. Moreover, whenever $\langle V\rangle \leq 1.9$, the Cepheid would be too bright (unrealistic apparent magnitude) and then rejected. The number of simulated Cepheids is then almost equal to the true one.

In order to show that the simulated sample is comparable to the true HIPPARCOS one, we plot for one simulated sample the same figures (Fig. 5 to 13) as those produced with the true HIPPARCOS sample. Note that the figures from the simulated sample are made from a single drawing which is not necessarily an optimal representation of the true sample.

4 RESULTS

The result may depend on the particular sample we draw. In order to reduce the uncertainty due to this choice, we made 1000 different random drawings (each of them with about 240 Cepheids) and adopted the mean result. We obtain the result shown in the table 2 (let us recall that the input zero-point is $\rho_V = -1.30$).

The simulation clearly confirms that the weighting in $(\sigma_{\pi_i}/\pi_i)^{-2}$ is meaningless. Again, it is confirmed that a cut in magnitude gives more stable results because the method of averaging $10^{0.2\rho}$ to get ρ is better justified with small dispersion. This answers the second question of section 1. The simulation also confirms that the FC weighting leads to the lowest dispersion and that the results are too low at only a 0.02 or 0.01 mag. level.

In order to analyze the effect of the measurement errors, we progressively reduce the observational errors (but not the intrinsic dispersion) introduced in our simulation. The reduction is made from their realistic values down to zero. We compute the mean value of the distribution of ρ as we go along, and plot the results in figure 3. It appears that the zero-point values comes closer to the real value $\rho = -1.30$. Moreover, the FC weighting gives clearly the more stable result. The trends of figure 3 (decreasing of ρ with increasing errors) can be explained solely by errors on π_i because they disappear when σ_{π_i} is forced to zero.

Further, we checked that removing both the measurement errors and the intrinsic dispersion removes the residual shift for all kinds of weighting and gives back the initial value

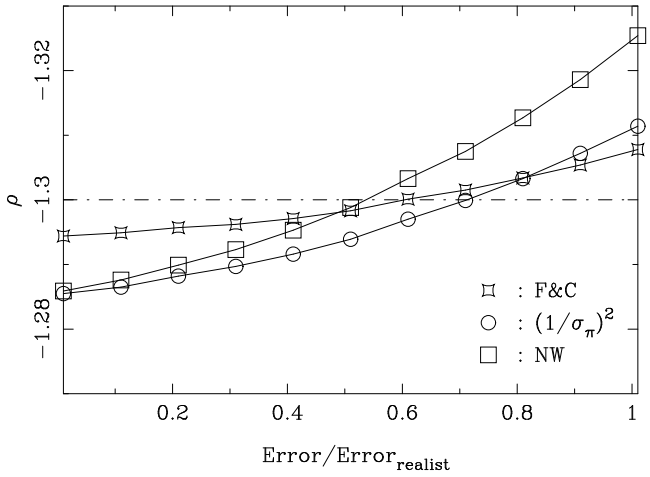

Figure 3. Zero-point values for each weighting when the observational error is progressively reduced from its realist value down to zero.

$\rho = -1.30$. This proves that our simulation procedure works well.

5 DISCUSSION

The results of the previous section allow us to answer the questions of section 1: a cut in apparent magnitude reduces the dispersion and gives reliable results because averaging $10^{0.2\rho}$ works better with small dispersion. Whatever the weighting adopted, the zero-point is not biased by more than 0.03 mag. The FC weighting gives the smallest standard deviation, and the systematic shift never exceeds 0.01 mag.

Let us analyze the main effects which are responsible for a shift. Two effects are present: effect of averaging in $10^{0.2\rho}$ and Malmquist effect. We will see that they work in two opposite directions.

Consider two Cepheids comparable in every aspect, i.e. located at the same distance in two directions with the same interstellar absorption, measured with the same σ_π so that they have the same observed parallaxes, and both with the same periods, but one located near one edge of the instability strip whereas the second is located at the opposite edge. Their absolute magnitudes would then be:

$$\langle M_V^1 \rangle = \delta \log P + \rho + \zeta \tag{16}$$

$$\langle M_V^2 \rangle = \delta \log P + \rho - \zeta \tag{17}$$

where ζ is the actual value of the intrinsic dispersion ($\langle \Delta \rangle = 0$; $\sigma(\Delta) \approx 0.2$) across the instability strip.
When using these two Cepheids to compute the zero-point of the PL relation directly from the parallax we would obtain:

$$\rho_1 = \langle V_0 \rangle + \zeta' + 5 \log \pi - 10 - \delta \log P \tag{18}$$

$$\rho_2 = \langle V_0 \rangle - \zeta' + 5 \log \pi - 10 - \delta \log P \tag{19}$$

with $\zeta' \leq \zeta$ because of dereddening method. The mean of the two values corresponds then to the true value ρ since:

$$\frac{\rho_1 + \rho_2}{2} = \rho_{true} \tag{20}$$

However we have shown why such a direct mean cannot be used with HIPPARCOS data. So we compute the mean (or the weighted mean) of the two quantities $10^{0.2\rho_1}$ and $10^{0.2\rho_2}$. The mean zero-point $\overline{\rho}$ can be expressed as:

$$\overline{\rho} = \rho_{true} + 5 \ \log[\frac{\omega_1/\omega_2 10^{0.2\zeta'} + 10^{-0.2\zeta'}}{1 + \omega_1/\omega_2}] \tag{21}$$

where ω_1 and ω_2 are the weights of the two quantities.

If we adopt $\omega_1/\omega_2 = 1$ (i.e. no weighting or same weights) and $\zeta' = 0.2$ (overvalued in order to highlight the way ρ is biased) we obtain $\overline{\rho} = \rho_{true} + 0.01$. The observed ρ slighly increases in this manner.

The Malmquist effect works in the other direction. The biased absolute magnitude $\overline{M'}$ is too bright (Teerikorpi 1984) :

$$\overline{\langle M' \rangle} = \overline{\langle M \rangle} - 1.38\sigma^2 \tag{22}$$

where $\overline{\langle M \rangle}$ is the unbiased magnitude. This formula gives the global correction, not the correction for individual Cepheid. Assuming a pessimistic value $\sigma = 0.2$ (once again, since the use of the PC relation as a narrowing effect, σ is surely lower than this value) the shift would be at worst -0.055. Then the observed ρ diminishes.

Finally, the net shift would be -0.04 or less. However, figure 3 which reproduces both effects with realistic uncertainties gives a shift of $\rho_{observed} = \rho_{true} - 0.01$ when the FC weighting is used. This shift takes in account these two effects. One will then apply it on the value deduced from HIPPARCOS data.

We investigate now the effect of a change in the adopted slope. We adopted $\delta = -2.77 \pm 0.08$. What would be the change in the PL relation if the true slope was different from this value? In table 3 we give the values of the mean $\langle M_V \rangle$ deduced from our simulation, the input relations being :

$$\langle M_V \rangle + 4.07 = -2.77(\log P - 1) \tag{23}$$

or

$$\langle M_V \rangle + 3.74 = -2.77(\log P - 0.88) \tag{24}$$

We note that the absolute magnitude at $\log P = 1$ (or $\log P = 0.88$) doesn't change very much (less than 0.03) as far as the $\log P$ does not change from the mean of calibrating Cepheids.

Table 3. Effect of the chosen slope on the final magnitudes computed at the mean $\log P$ (0.88) and at $\log P = 1$

slope	$\langle M_V \rangle$ at $\log P$ mean	$\langle M_V \rangle$ at 10 d
-2.60	-3.76	-4.07
-2.70	-3.75	-4.08
-2.77	-3.75	-4.08
-2.80	-3.75	-4.08
-2.90	-3.74	-4.09
-3.00	-3.74	-4.10
Reference values		
-2.77	-3.74	-4.07

6 CONCLUSION

The conclusion is that the intrinsic dispersion (even Gaussian and symetrical) of the instability strip is responsible for too low values of ρ and may lead to a slightly biased result as long as the zero-point ρ is deduced by averaging $10^{0.2\rho}$. However it is compensated by the Malmquist bias, and, using a PC relation for dereddening the individual Cepheids, the final effect is globally very small. Indeed, our simulation shows that it is almost negligible (Fig. 3) even when we account for measurement errors. With realistic measurement errors the bias is about -0.01. A cut in apparent magnitude reduces the uncertainty on the zero-point. The best unbiased zero-point is obtained by cutting the sample at $V \leq 5.5$ mag. The result is (after correction of the residual shift of -0.01):

$$\rho = -1.44 \pm 0.05 \qquad (n = 11) \tag{25}$$

for a slope $\delta_V = -2.77 \pm 0.08$ and a weighted mean $\langle \log P \rangle = 0.82$. The adopted V-band PL relation is then $\langle M_V \rangle = -2.77 \pm 0.08 \ \log P - 1.44 \pm 0.05$ or $\langle M_V \rangle + 4.21 = -2.77 \ (\log P - 1)$.

ACKNOWLEDGEMENTS

We thank L. Szabados for communicating his list of binary Cepheids and the referee for his valuable comments.

APPENDIX A

At present, the Hubble Space Telescope has observed Cepheids in 19 galaxies (see Lanoix et al. 1999b for an extensive compilation). These observations are made in two bandpasses (V and I), so that we need a calibration of the PL relation both in V and I to apply a dereddening procedure (see Freedman et al. 1994, for instance) and compute the distance moduli of these galaxies.

With this aim in view for a future paper, we then perform the I calibration based on HIPPARCOS parallaxes in the light of our V calibration. The major problem is that there's no homogeneous I photometry available for each Cepheid of the calibrating sample, and that a selection may induce a biased result. As a matter of fact we found I (Cousins) photometry for 174 Cepheids of the sample from Caldwell & Coulson (1987). We apply to these values a tiny correction (0.03 mag) in order to convert them into intensity averaged magnitudes. The I magnitudes of these stars are listed in table 4 when available. Since the selection doesn't come from a rough cut in the HIPPARCOS sample, it will not necessarily lead us to a biased result. We then apply the same selection to the V sample and compute again the visual zero-point. From these 174 cepheids we obtain:

$$\rho = -1.49 \pm 0.10 \tag{26}$$

This result is almost identical to the one obtained with the complete sample (Eq. 25), so that we conclude that this selection implies a little bias of 0.04 with respect to the complete sample and only 0.05 with respect to the adopted final value. We will take it into account to determine the associated I zero-point.

The residuals of the I and the V PL relations are correlated so that we will apply the same procedure as we do for the V band and obtain the same narrowing effect of the instability strip. We then need the slope of the I PL relation as well as the I ratio of total to selective absorption. Concerning the slope that is well determined, we choose $\delta_I = -3.05$ (see Gieren et al. 1998, Madore & Freedman 1991 for instance). Let's recall that the influence of a variation of the slope is very weak. Concerning R_I, we choose according to Caldwell & Coulson (1987):

$$R_I = 1.82 + 0.20(\langle B \rangle_0 - \langle V \rangle_0) + 0.02 E_{(B-V)} \tag{27}$$

The calculus leads to :

$$\rho_I = -1.84 \pm 0.09 \tag{28}$$

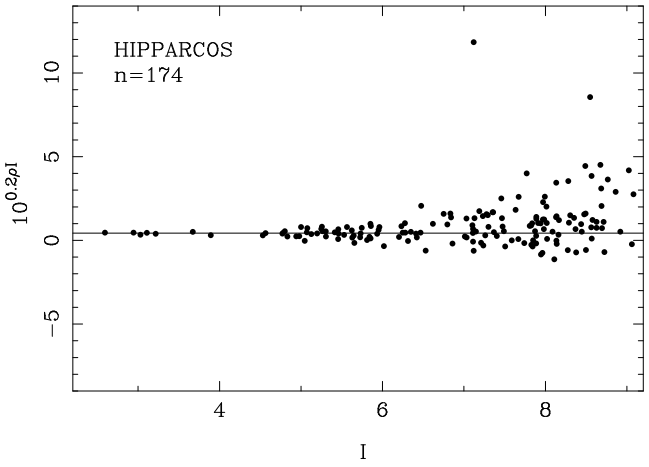

Figure 4. Position of the 174 remaining Cepheids in the I diagram zero-point vs. magnitude. The horizontal line corresponds to $\rho_I = -1.84$.

Figure 4 shows that these 174 Cepheids still have an almost symetrical distribution around a mean value, and that only faint stars with low weights have been rejected from the sample. That may explain why the result is only slightly biased.

Keeping in mind that the instability strip is narrower in I than in V band, the bias du to the selection of this sample should be less than 0.04 mag. Finally we adopt:

$$\rho_I = -1.81 \pm 0.09 \tag{29}$$

for a slope $\delta_I = -3.05$.

APPENDIX B

We also investigated the effect of binarity as pointed out by Szabados (1997). We indeed found that the dispersion of the zero-point is reduced when only non-binary Cepheids are used. However, we interpreted this effect by the fact that confirmed non-binary Cepheids are brighter. Actually, using either non-binary (Evans 92) or binary (Szabados private communication) Cepheids does not affect significantly the value of the zero-point.

REFERENCES

Alcock C., et al., 1995, AJ, 109, 1653

Brown A. G. A., Arenou F., van Leeuwen F., Lindegren L., Luri X., proceedings of the ESA Symposium 'HIPPARCOS Venice 97', Venice, Italy, ESA SP-402 (July 1997), p63
Caldwell J. A. R., Coulson I. M., 1987, AJ, 93, 1090
Caldwell J. A. R., Coulson I. M., 1991, in Haynes R., Milne D., (eds.), The Magellanic Clouds, (IAU Symposium 148) Kluwer; Dordrecht, p. 249
Evans N.R., 1992, ApJ, 384, 220
Feast M. W., Catchpole R. M., 1997, MNRAS, 286, L1
Fernie J. D., Beattie B., Evans N. R., Seager S., 1995, IBVS No. 4148
Freedman W. L., et al., 1994, ApJ, 427, 628
Gieren W. P., Fouqué P., Gómez M., 1998, ApJ, 496, 17
The HIPPARCOS Catalogue, 1997, ESA SP-1200
Laney C. D., Stobie R. S., 1993, MNRAS, 263, 921
Laney C. D., Stobie R. S., 1994, MNRAS, 266, 441
Lanoix P., Paturel G., Garnier R., 1999a, ApJ, 516 (in press)
Lanoix P., Paturel G., Garnier R., Petit, C., Rousseau, J., Di Nella-Courtois, H., 1999b, Astron. Nach. 220, 320, 21
Lutz T. E., Kelker D. H., 1973, PASP, 85, 573
Madore B. F., Freedman W., 1991, PASP, 103, 933
Madore B. F., Freedman W., 1998, ApJ, 492, 110
Malmquist K. G., 1920, Lund. Astron. Obs. Ser 2., 22
Paturel G., Bottinelli L., Garnier R., Gouguenheim L., Lanoix P., Rousseau J., Theureau G., Turon C., 1996, C. R. Acad. Sci. Paris, t. 323, Série II b
Paturel G., Lanoix P., Garnier R., Rousseau J., Bottinelli L., Gouguenheim L., Theureau G., Turon C., proceedings of the ESA Symposium 'HIPPARCOS Venice 97', Venice, Italy, ESA SP-402
Sandage A., Tammann G. A., MNRAS, 293, L23
Szabados L., proceedings of the ESA Symposium 'HIPPARCOS Venice 97', Venice, Italy, ESA SP-402
Tanvir N., 1997 Proceedings of the STScI symposium of the 'Extragalactic Distance Scale'
Teerikorpi P., 1984, A&A, 141, 407

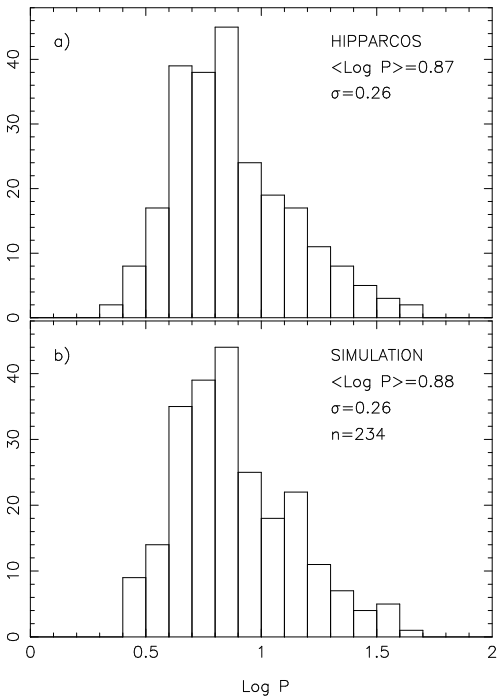

Figure 5. Histograms of $\log P$ for HIPPARCOS data and for a simulated sample. In Figure a, the periods of overtone pulsators are corrected (see text).

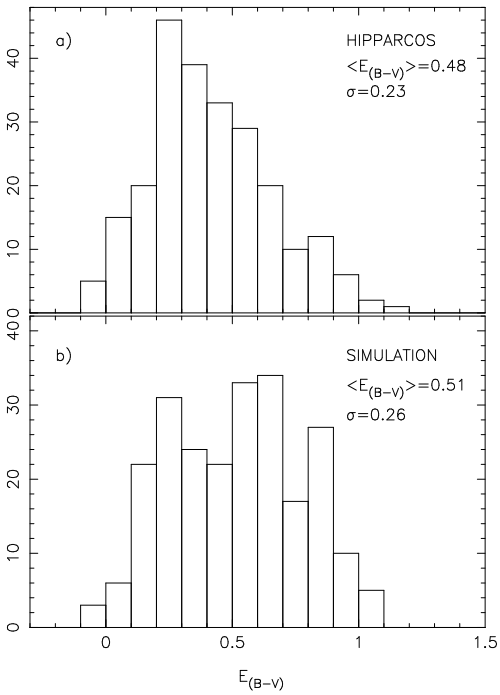

Figure 6. Histograms of observed $E_{(B-V)}$ for HIPPARCOS data and for a simulated sample according to equations 4 and 14 respectively.

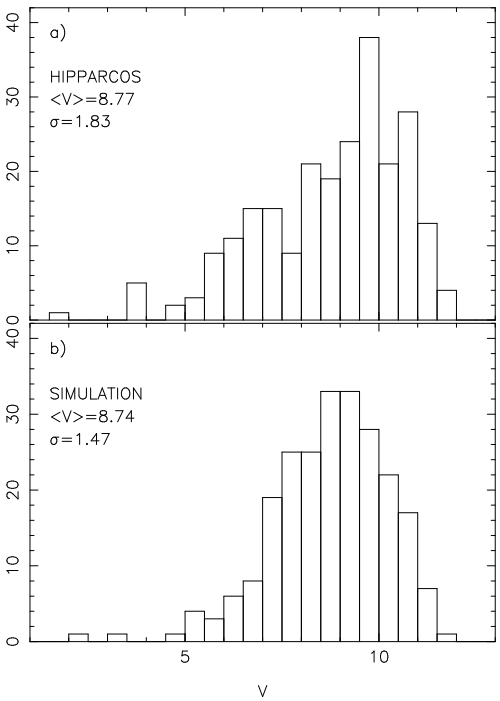

Figure 7. Apparent V magnitudes for HIPPARCOS data and for a simulated sample.

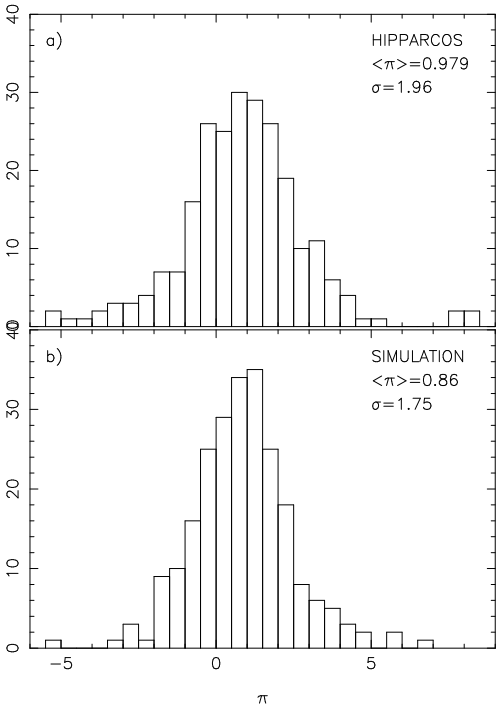

Figure 8. Observed parallaxes π in mas for HIPPARCOS data and for a simulated sample.

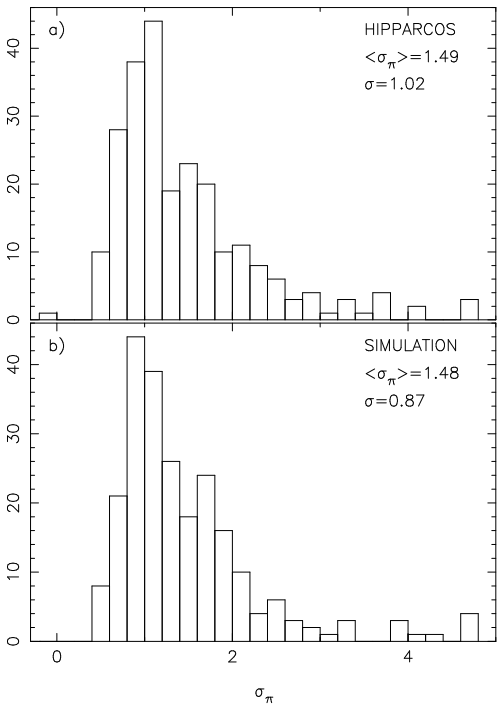

Figure 9. Errors on the observed parallaxes for HIPPARCOS data and for a simulated sample.

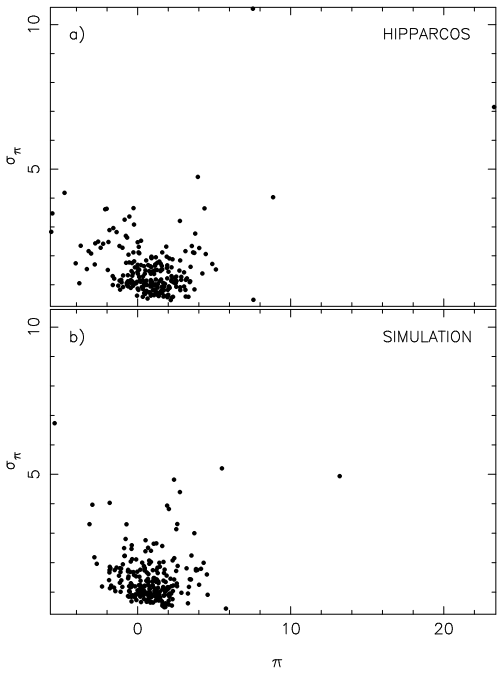

Figure 10. σ_π vs. π for HIPPARCOS data and for a simulated sample. The two quantities are not correlated.

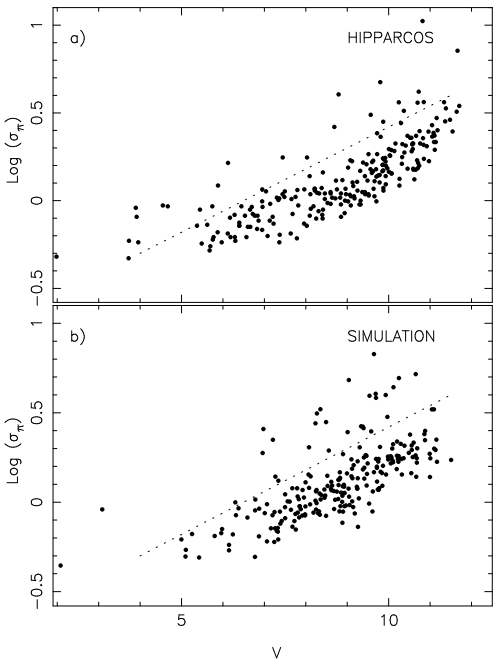

Figure 11. $\log \sigma_\pi$ vs. V for HIPPARCOS data and for a simulated sample. We can see the two populations of Cepheids as described in the text.

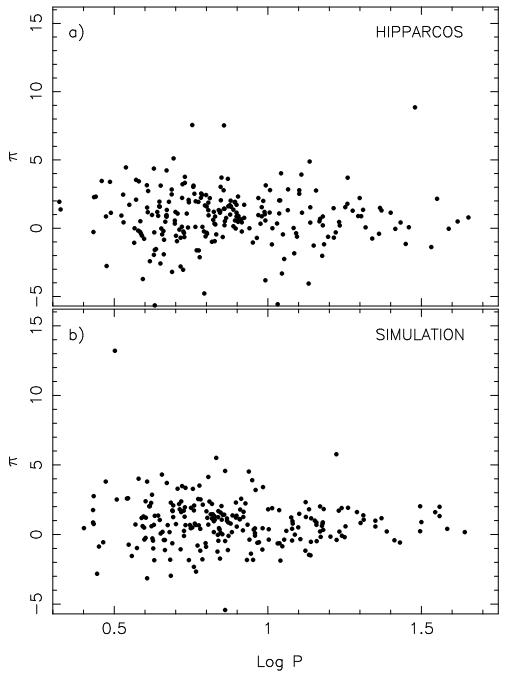

Figure 12. π vs. $\log P$ for HIPPARCOS data and for a simulated sample. It shows that there's no correlation between these two quantities.

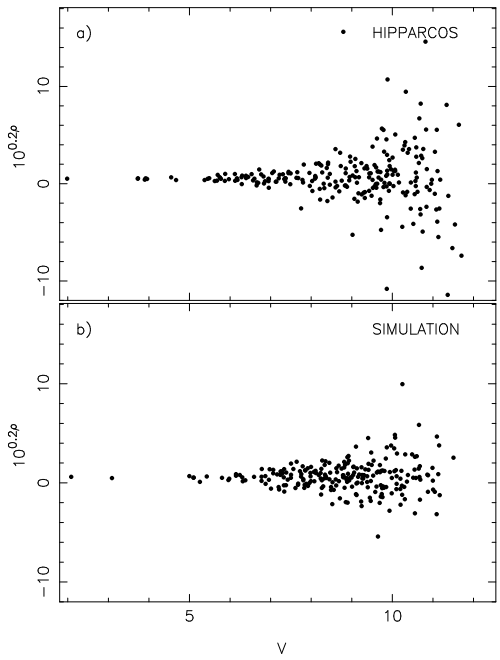

Figure 13. The distribution of the exposant of the zero-points is plotted as a function of the apparent V-magnitude for both HIPPARCOS data and a simulated sample. Note that figure a is the same than figure 1.

Table 4: The 238 Cepheids from HIPPARCOS.

Name	logPo	Pi	Sig_pi	<V>	<B>	<I>
eta Aql	.856	2.78	.91	3.897	4.686	3.029
FF Aql	.806	1.32	.72	5.372	6.128	4.531
FM Aql	.786	2.45	1.11	8.270	9.547	6.797
FN Aql	1.138	1.53	1.18	8.382	9.596	7.030
SZ Aql	1.234	.20	1.10	8.599	9.988	7.032
TT Aql	1.138	.41	.96	7.141	8.433	5.725
V336 Aql	.864	.75	1.47	9.848	11.160	8.369
V493 Aql	.475	-2.77	2.43	11.083	12.363	
V496 Aql	.992	-3.81	1.05	7.751	8.897	6.475
V600 Aql	.859	1.42	1.80	10.037	11.499	8.288
V1162 Aql	.888	.15	1.15	7.798	8.688	
U Aql	.847	2.05	.93	6.446	7.470	5.264
V340 Ara	1.318	.06	2.12	10.164	11.703	8.568
AN Aur	1.013	-1.19	2.34	10.455	11.673	
BK Aur	.903	.47	1.38	9.427	10.489	
RT Aur	.571	2.09	.89	5.446	6.041	4.772
RX Aur	1.065	1.32	1.02	7.655	8.664	6.619
SY Aur	1.006	1.15	1.70	9.074	10.074	7.889
Y Aur	.587	-.40	1.47	9.607	10.518	
YZ Aur	1.260	3.70	2.10	10.332	11.707	
RW Cam	1.215	-.69	2.63	8.691	10.042	7.120
RX Cam	.898	1.14	.84	7.682	8.875	6.279
AQ Car	.990	1.02	.81	8.851	9.779	7.889
CN Car	.693	5.11	1.53	10.700	11.789	
CY Car	.630	-.30	1.40	9.782	10.735	
ER Car	.888	1.36	.69	6.824	7.691	5.953
EY Car	.459	3.46	1.62	10.318	11.172	
FN Car	.661	-1.91	2.48	11.542	12.643	
FR Car	1.030	.35	1.29	9.661	10.782	8.445
GH Car	.915	.43	1.03	9.177	10.109	8.088
GI Car	.802	-.41	1.10	8.323	9.062	7.505
GX Car	.857	1.43	1.12	9.364	10.407	8.136
GZ Car	.774	1.93	1.22	10.261	11.240	9.081
HW Car	.964	-.71	1.06	9.163	10.218	
IT Car	.877	1.00	.82	8.097	9.087	7.111
l Car	1.551	2.16	.47	3.724	5.023	2.593
SX Car	.687	2.48	1.06	9.089	9.976	8.013
U Car	1.589	-.04	.62	6.288	7.471	5.045
UW Car	.728	-.64	1.12	9.426	10.397	8.275
UX Car	.566	.00	.87	8.308	8.935	7.586
UZ Car	.716	-.70	1.00	9.323	10.198	8.376
V Car	.826	.34	.58	7.362	8.234	6.422
VY Car	1.276	1.28	1.76	7.443	8.614	6.275
WW Car	.670	4.23	1.39	9.743	10.633	8.675
WZ Car	1.362	-.41	1.14	9.247	10.389	7.946
XX Car	1.196	-.63	.95	9.322	10.376	8.108
XY Car	1.095	-.62	.95	9.295	10.509	7.963
XZ Car	1.221	-.30	.96	8.601	9.867	7.237
YZ Car	1.259	1.79	1.03	8.714	9.838	7.458
BP Cas	.797	-.60	2.04	10.920	12.470	
BY Cas	.662	-.85	3.25	10.366	11.645	
CD Cas	.892	1.91	1.58	10.738	12.187	
CF Cas	.688	-3.20	2.16	11.136	12.310	9.752
CH Cas	1.179	.21	1.68	10.973	12.623	
CY Cas	1.157	2.76	3.21	11.641	13.379	
DD Cas	.992	.57	1.14	9.876	11.064	8.562
DL Cas	.903	2.32	1.09	8.969	10.123	7.634
DF Cas	.584	-.27	3.65	10.848	12.029	
DW Cas	.699	1.19	1.95	11.112	12.587	
FM Cas	.764	.10	1.27	9.127	10.116	8.021
RS Cas	.799	2.43	1.24	9.932	11.422	
RW Cas	1.170	.69	1.68	9.117	10.213	7.910
RY Cas	1.084	.02	1.38	9.927	11.311	
SU Cas	.440	2.31	.58	5.970	6.673	5.127

Table 4: (continued)

Name	logPo	Pi	Sig_pi	<V>	<B>	<I>
SW Cas	.736	1.07	1.37	9.705	10.786	8.439
SY Cas	.610	2.73	1.49	9.868	10.860	
SZ Cas	1.299	2.21	1.60	9.853	11.272	8.133
UZ Cas	.629	4.37	3.64	11.338	12.448	
V636 Cas	.923	1.72	.81	7.199	8.564	
VV Cas	.793	-4.78	4.18	10.724	11.867	
VW Cas	.778	-2.12	3.61	10.697	11.942	
XY Cas	.653	-.02	1.58	9.935	11.082	
AY Cen	.725	-.24	1.04	8.830	9.839	7.740
AZ Cen	.660	-.20	1.04	8.636	9.289	7.887
BB Cen	.757	3.03	1.43	10.073	11.026	9.023
KK Cen	1.086	-1.84	2.89	11.480	12.762	9.962
KN Cen	1.532	-1.38	2.82	9.870	11.452	7.992
V Cen	.740	.05	.82	6.836	7.711	5.810
V339 Cen	.976	.33	1.16	8.753	9.944	7.404
V378 Cen	.969	.96	1.02	8.460	9.495	7.301
V419 Cen	.898	1.72	.93	8.186	8.944	7.351
V496 Cen	.646	1.61	1.53	9.966	11.138	8.579
V737 Cen	.849	3.71	.84	6.719	7.718	
VW Cen	1.177	-2.02	3.63	10.245	11.590	8.766
XX Cen	1.040	2.04	.94	7.818	8.801	6.750
AK Cep	.859	.22	2.52	11.180	12.521	
IR Cep	.325	1.38	.61	7.784	8.672	
CR Cep	.795	1.67	1.06	9.656	11.052	8.017
CP Cep	1.252	1.54	1.52	10.590	12.258	
del Cep	.730	3.32	.58	3.954	4.611	3.217
AV Cir	.486	3.40	1.09	7.439	8.349	
AX Cir	.722	3.22	1.22	5.880	6.621	5.000
RW CMa	.758	3.12	2.16	11.096	12.321	
RY CMa	.670	.96	1.09	8.110	8.957	7.146
RZ CMa	.629	-1.95	1.51	9.697	10.701	8.494
SS CMa	1.092	-.37	1.75	9.915	11.127	8.497
TV CMa	.669	.90	1.97	10.582	11.757	
TW CMa	.845	1.26	1.51	9.561	10.531	8.475
VZ CMa	.648	1.58	1.65	9.383	10.340	8.166
AD Cru	.806	1.87	2.32	11.051	12.330	
BG Cru	.678	1.94	.57	5.487	6.093	4.781
R Cru	.765	1.97	.82	6.766	7.538	5.963
S Cru	.671	1.34	.71	6.600	7.361	5.731
SU Cru	1.109	3.93	4.73	9.796	11.548	7.672
T Cru	.828	.86	.62	6.566	7.488	5.647
CD Cyg	1.232	.46	1.00	8.947	10.213	7.490
DT Cyg	.549	1.72	.62	5.774	6.312	5.197
GH Cyg	.893	1.93	1.67	9.924	11.190	
MW Cyg	.775	-1.63	1.30	9.489	10.805	7.941
SU Cyg	.585	.51	.77	6.859	7.434	6.203
SZ Cyg	1.179	.86	1.09	9.432	10.909	7.825
TX Cyg	1.168	.50	1.09	9.511	11.295	7.262
V386 Cyg	.721	2.22	1.17	9.635	11.126	7.836
V402 Cyg	.640	1.19	1.18	9.873	10.881	8.714
V459 Cyg	.860	.51	1.50	10.601	12.040	8.919
V495 Cyg	.827	-.95	1.32	10.621	12.244	
V520 Cyg	.607	1.51	1.73	10.851	12.200	
V532 Cyg	.670	.84	.94	9.086	10.122	7.872
V538 Cyg	.787	.10	1.52	10.456	11.739	
V924 Cyg	.903	.83	1.64	10.710	11.557	9.760
V1334 Cyg	.523	.93	.66	5.871	6.375	5.305
VX Cyg	1.304	.88	1.43	10.069	11.773	
VY Cyg	.895	-.02	1.44	9.593	10.808	8.134
VZ Cyg	.687	2.84	1.17	8.959	9.835	7.971
X Cyg	1.214	1.47	.72	6.391	7.521	5.249
bet Dor	.993	3.14	.59	3.731	4.538	2.944
AA Gem	1.053	-2.25	2.42	9.721	10.782	8.566
AD Gem	.578	-.18	1.60	9.857	10.551	9.061

Table 4: (continued)

Name	logPo	Pi	Sig_pi	<V>	<B>	<I>
DX Gem	.650	-2.58	2.49	10.746	11.682	9.622
RZ Gem	.743	1.90	1.97	10.007	11.032	8.688
W Gem	.898	.86	1.16	6.950	7.839	5.935
zet Gem	1.007	2.79	.81	3.918	4.716	3.108
BG Lac	.727	-.35	1.31	8.883	9.832	7.827
RR Lac	.807	.94	.95	8.848	9.733	7.807
V Lac	.697	.34	.85	8.936	9.809	7.887
X Lac	.893	.57	.79	8.407	9.308	7.368
Y Lac	.636	-1.53	1.21	9.146	9.877	8.305
Z Lac	1.037	2.04	.89	8.415	9.510	7.188
V473 Lyr	.321	1.94	.62	6.182	6.814	5.528
AC Mon	.904	.90	1.94	10.067	11.232	8.628
BE Mon	.432	-.28	2.12	10.578	11.712	
CV Mon	.730	3.76	2.77	10.299	11.596	8.684
EK Mon	.597	-.77	2.69	11.048	12.243	
SV Mon	1.183	-1.18	1.14	8.219	9.267	7.130
T Mon	1.432	.42	1.64	6.124	7.290	4.978
TX Mon	.940	.00	2.47	10.960	12.056	9.661
TZ Mon	.871	1.61	2.12	10.761	11.877	
V465 Mon	.434	2.28	1.88	10.379	11.141	
V508 Mon	.616	-2.42	2.28	10.518	11.416	
V526 Mon	.580	3.43	1.12	8.597	9.190	
R Mus	.876	1.69	.59	6.298	7.055	5.457
RT Mus	.489	1.13	.99	9.022	9.856	7.981
S Mus	.985	2.00	.65	6.118	6.951	5.257
UU Mus	1.066	2.85	1.27	9.781	10.931	8.489
GU Nor	.538	4.45	2.06	10.411	11.684	8.861
IQ Nor	.915	-.24	3.08	9.566	10.880	8.139
RS Nor	.792	-.23	1.81	10.027	11.314	
S Nor	.989	1.19	.75	6.394	7.335	5.414
SY Nor	1.102	2.78	1.84	9.513	10.853	
TW Nor	1.032	-5.57	3.47	11.704	13.634	9.339
U Nor	1.102	2.52	1.28	9.238	10.814	7.358
BF Oph	.609	1.17	1.01	7.337	8.205	6.411
Y Oph	1.400	1.14	.80	6.169	7.546	4.564
CS Ori	.590	-.54	3.36	11.381	12.305	
RS Ori	.879	2.02	1.45	8.412	9.357	7.278
AS Per	.697	.56	1.84	9.723	11.025	8.160
AW Per	.811	2.20	1.13	7.492	8.547	6.232
SV Per	1.046	-3.32	1.54	9.020	10.049	7.769
SX Per	.632	-1.59	2.96	11.158	12.313	
V440 Per	.879	1.62	.83	6.282	7.155	5.303
VX Per	1.037	1.08	1.48	9.312	10.470	7.969
UX Per	.660	23.29	7.15	11.664	12.691	
AD Pup	1.133	-4.05	1.74	9.863	10.912	
AP Pup	.706	1.07	.64	7.371	8.209	6.467
AQ Pup	1.479	8.85	4.03	8.791	10.214	7.119
AT Pup	.824	1.20	.74	7.957	8.740	7.103
BM Pup	.857	7.53	10.55	10.817	12.022	
BN Pup	1.136	4.88	1.72	9.882	11.068	8.549
EK Pup	.571	3.54	2.34	10.664	11.480	
MY Pup	.913	.65	.52	5.677	6.308	4.941
RS Pup	1.618	.49	.68	6.947	8.340	5.461
VW Pup	.632	-5.65	2.83	11.365	12.430	
VZ Pup	1.365	1.49	1.47	9.621	10.783	8.280
WW Pup	.742	2.07	1.91	10.554	11.428	
WX Pup	.951	-1.05	1.08	9.063	10.031	7.985
WY Pup	.720	.11	2.09	10.569	11.360	9.747
WZ Pup	.701	-.55	1.77	10.326	11.115	9.408
X Pup	1.415	-.05	1.10	8.460	9.587	7.111
KQ Sco	1.459	.07	2.31	9.807	11.741	7.667
RV Sco	.783	2.54	1.13	7.040	7.995	5.857
V482 Sco	.656	-.45	1.16	7.965	8.940	6.859

Table 4: (continued)

Name	logPo	Pi	Sig_pi	<V>	<B>	<I>
V500 Sco	.969	2.21	1.30	8.729	10.005	7.232
V636 Sco	.832	-.45	.89	6.654	7.590	5.655
V950 Sco	.529	2.46	1.04	7.302	8.077	
CK Sct	.870	3.62	2.12	10.590	12.156	
CM Sct	.593	-3.72	2.35	11.106	12.477	9.479
EV Sct	.643	.91	1.92	10.137	11.297	8.694
RU Sct	1.294	.89	1.61	9.466	11.111	7.474
SS Sct	.565	-1.07	1.17	8.211	9.155	7.110
TY Sct	1.043	4.02	2.27	10.831	12.488	
X Sct	.623	.97	1.46	10.006	11.146	8.628
Y Sct	1.015	.00	1.69	9.628	11.167	7.849
Z Sct	1.111	1.14	1.66	9.600	10.930	8.131
CR Ser	.724	-3.04	2.08	10.842	12.486	
S Sge	.923	.76	.73	5.622	6.427	4.832
AP Sgr	.704	-.95	.92	6.955	7.762	6.018
AY Sgr	.818	-.99	2.28	10.549	12.006	
BB Sgr	.822	.61	.99	6.947	7.934	5.840
U Sgr	.829	.27	.92	6.695	7.782	5.455
V350 Sgr	.712	-.10	1.05	7.483	8.388	6.314
W Sgr	.880	1.57	.93	4.668	5.414	3.892
WZ Sgr	1.340	-.75	1.76	8.030	9.422	6.530
X Sgr	.846	3.03	.94	4.549	5.288	3.671
Y Sgr	.761	2.52	.93	5.744	6.600	4.801
YZ Sgr	.980	.87	1.03	7.358	8.390	6.248
EU Tau	.473	.86	1.38	8.093	8.757	
ST Tau	.606	3.15	1.17	8.217	9.064	
SZ Tau	.651	3.12	.82	6.531	7.375	5.564
S TrA	.801	1.59	.72	6.397	7.149	5.623
R TrA	.530	.43	.71	6.660	7.382	5.853
alf UMi	.754	7.56	.48	1.982	2.580	1.393
AE Vel	.853	-.64	1.33	10.262	11.505	8.723
AH Vel	.782	2.23	.55	5.695	6.274	5.078
BG Vel	.840	1.33	.65	7.635	8.810	6.348
DR Vel	1.049	-.45	1.07	9.520	11.038	7.842
RY Vel	1.449	-1.15	.83	8.397	9.749	6.841
RZ Vel	1.310	1.35	.63	7.079	8.199	5.852
ST Vel	.768	-1.62	.99	9.704	10.899	8.351
SV Vel	1.149	-1.27	.97	8.524	9.758	7.466
SW Vel	1.370	1.30	.90	8.120	9.282	6.834
SX Vel	.980	1.54	.79	8.251	9.139	7.293
T Vel	.666	.48	.72	8.024	8.946	7.010
XX Vel	.844	1.14	1.50	10.654	11.816	
BR Vul	.716	-2.80	1.70	10.687	12.161	
SV Vul	1.653	.79	.74	7.220	8.662	5.746
T Vul	.647	1.95	.60	5.754	6.389	5.071
U Vul	.903	.59	.77	7.128	8.403	5.630
X Vul	.801	-.33	1.10	8.849	10.238	7.210